

# Dynamic Analysis and Controller Design for the Ballbot

Zhuang He<sup>1</sup>, Liang Yan<sup>\*1,2</sup>, Xiaoshan Gao<sup>1</sup>, Chris Gerada<sup>3</sup>

<sup>1</sup> School of Automation Science and Electrical Engineering, Beihang University, Beijing, 100089, China

<sup>2</sup> Ningbo Institute of Technology, Beihang University, Ningbo, 315300, China

<sup>3</sup> Department of Electrical and Electronic Engineering, University of Nottingham, Nottingham, 999020, U.K.

hezhuang2018@buaa.edu.cn, lian1991@gmail.com, gaoshan0920@buaa.edu.cn, chris.gerada@nottingham.ac.uk

**Abstract**—A ballbot is a dynamically stable mobile robot that shows the capability of omnidirectionality, agility, and maneuverability on a floor. This paper presents the design prototype and control scheme of a ballbot. By assuming that the effected noise is white gaussian noise, a Kalman estimator is applied to estimate the internal state of the system. To improve the trajectory tracking performance of the ballbot, a Linear Quadratic Tracking (LQT) controller is designed to balance and transfer the ballbot system taking into account the presence of the noise in system, and the numerical simulation results imply the correctness of the system modeling and effectiveness of LQT control design for a MIMO ballbot system.

**Keywords**—ballbot, Lagrangian method, LQT control, Kalman filter

## I. INTRODUCTION

With the rapid development of technology, the mobile robots used in indoor environments such as home automation, industrial space, and healthcare are strongly developed. Recently, the ballbot has gradually came into people's sight. Due to the capability of agility, omnidirectionality, and maneuverability on a floor<sup>[1-4]</sup>, ballbot can be applied in various fields of automatic control and robotics areas. As a spatial spherical wheeled inverted pendulum robot, it adjusts attitude by driving the ball<sup>[5]</sup>.

The first ballbot was developed by at Carnegie Mellon University in 2006, and it was actuated by a pair of stainless steel rollers placed orthogonally at the sphere's equator<sup>[6]</sup>. Although the robot could move in all directions, it could not rotate around yaw axis. In 2008, 'BallIP' that firstly utilized three omni-wheels as driving mechanism was invented at Thoku Gakuin University<sup>[7]</sup>, and the structure allow it to rotate around yaw axis. Dinh Ba Pham et.al created a spatial rideable ballbot at Kyung Hee University in 2018, which was designed for transporting a person, so it's bigger than other ballbot. Simulation results demonstrated that the robot could asymptotically reach destinations and had good robustness under the large disturbance<sup>[8]</sup>.

There are two control objectives for ballbot, namely maintaining the balancing of the body around its upright unstable equilibrium and transferring the system to follow a given trajectory. Lots of studies are investigated for both modeling and control scheme design recently<sup>[9-10]</sup>. By the use of the linearized model, several studies are conducted based on linear quadratic regulator(LQR) control theory that can be applied to multiple-input and multiple-output(MIMO) systems. To improve the trajectory tracking performance of the ballbot, LQT controller is proposed in this paper.

The remainder of this paper is organized as follows. Section II is devoted to the modeling of the ballbot. Section

III describes the design of control scheme. In section IV, some numerical simulation results are discussed. Finally, the conclusion drawn from this work are given..

## II. SYSTEM MODELING

Fig.1 demonstrates the prototype of the ballbot, and it's segmented into two parts: ball and body. The body includes omni-wheel, DC motor, reducer, encoder, motor driver and controller. Due to the complexity of the robot, some assumptions that facilitate the system modeling need to be made: (1)The ball, body and floor are rigid. (2)No slip occurs between the ball and the omni-wheels, and the ball and the floor. (3)The floor is horizontal. (4)The contacts between the ball and the omi-wheels and between the floor and the ball are always point contacts.



Fig. 1. Developed the ballbot prototype.

To model the ballbot in the Euler-Lagrange formalism, coordinates need to be defined. The robot has five degree of the freedoms (DOFs), namely three DOFs for the rotation of the body and two DOFs for translation of the ball. Therefore, the minimal coordinate vector is defined as  $\mathbf{q} = [x_s \ y_s \ \varphi_z \ \varphi_y \ \varphi_x]^T$ , where  $x_s$  and  $y_s$  indicate the translation of the ball along the  $x$ - and  $y$ -axis respectively, and  $\varphi_z$ ,  $\varphi_y$  and  $\varphi_x$  indicate the orientation of the body. As shown in Fig.2, define the following five coordinate frames:

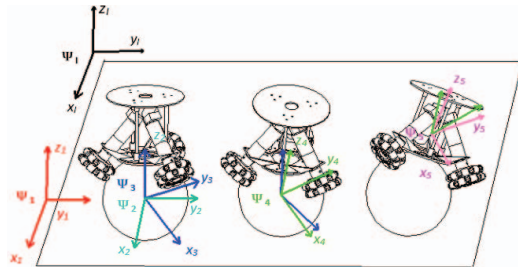


Fig. 2. Coordinate systems of the ballbot.

- The inertial frame of reference is denoted as  $I$ .
- Coordinate frame 1 is obtained by translating the inertial frame with  $x_s$  along its  $x$ -axis.
- Coordinate frame 2 is obtained by translating coordinate frame 1 with  $y_s$  along its  $y$ -axis, and the origin of coordinate frame 2 is at the center of the ball.
- Coordinate frame 3 is derived from rotating coordinate frame 2 around its  $z$ -axis with an angle  $\varphi_z$  counterclockwise.
- Coordinate frame 4 is obtained by rotating coordinate frame 3 around its  $y$ -axis with an angle  $\varphi_y$  counterclockwise.
- Coordinate frame 5 is derived from rotating coordinate frame 4 around its  $x$ -axis with an angle  $\varphi_x$  clockwise, and the origin of coordinate frame 5 is at the center of the mass(COM) of the body.

Dynamic analysis of the robot is based on the Lagrangian method, and the Euler-Lagrange equations can be expressed as follows:

$$\frac{d}{dt} \left( \frac{\partial T}{\partial \dot{\mathbf{q}}_i} \right) - \frac{\partial T}{\partial \mathbf{q}_i} + \frac{\partial V}{\partial \mathbf{q}_i} = \boldsymbol{\tau}_{ext} \quad (1)$$

where  $\boldsymbol{\tau}_{ext}$  is the external torques of the model.  $T$  and  $V$  are kinetic energy and potential energy of the ballbot, they are defined as :

$$T = T_s + T_B + \sum_{i=1}^3 T_i \quad (2)$$

$$V = V_B \quad (3)$$

where  $T_s$ ,  $T_B$  and  $T_i$  respectively denoted as kinetic energies of the ball, the body, and the omni-wheel;  $V_B$  is the potential energy of the body.

Finally, the equations of motion can be written as follows:

$$M(\mathbf{q})\ddot{\mathbf{q}} + C(\mathbf{q}, \dot{\mathbf{q}})\dot{\mathbf{q}} + G(\mathbf{q}) = \boldsymbol{\tau}_{ext} \quad (4)$$

where the first term stands for the inertial forces, the second term describes the centrifugal and Coriolis forces, the third term describes the gravitational forces and the right-hand side stands for the external torques.

The state-space model can be derived by linearizing the equations of motion around the position the robot stands upright<sup>[11]</sup>. The state-space model can be written as:

$$\begin{aligned} \dot{\mathbf{x}} &= A \cdot \mathbf{x} + B \cdot \mathbf{u} \\ \mathbf{y} &= C \cdot \mathbf{x} \end{aligned} \quad (5)$$

where  $C$  is the 10-by-10 identity matrix, and the state vector and the input vector are defined as:

$$\mathbf{x} = [x_s \ \dot{x}_s \ y_s \ \dot{y}_s \ \varphi_z \ \dot{\varphi}_z \ \varphi_y \ \dot{\varphi}_y \ \varphi_x \ \dot{\varphi}_x]^T \quad (6)$$

$$\mathbf{u} = [\mathbf{u}_1 \ \mathbf{u}_2 \ \mathbf{u}_3]^T \quad (7)$$

It makes sense to linearize all states at zero, and by calculation in Mathematica, matrix  $A$  and  $B$  can be derived.

$$A = \begin{bmatrix} 0 & 1 & 0 & 0 & 0 & 0 & 0 & 0 & 0 & 0 \\ 0 & 0 & 0 & 0 & 0 & 0 & -9.17 & 0 & 0 & 0 \\ 0 & 0 & 0 & 1 & 0 & 0 & 0 & 0 & 0 & 0 \\ 0 & 0 & 0 & 0 & 0 & 0 & 0 & 0 & -9.17 & 0 \\ 0 & 0 & 0 & 0 & 0 & 1 & 0 & 0 & 0 & 0 \\ 0 & 0 & 0 & 0 & 0 & 0 & 0 & 0 & 0 & 0 \\ 0 & 0 & 0 & 0 & 0 & 0 & 0 & 1 & 0 & 0 \\ 0 & 0 & 0 & 0 & 0 & 0 & 17.03 & 0 & 0 & 0 \\ 0 & 0 & 0 & 0 & 0 & 0 & 0 & 0 & 0 & 1 \\ 0 & 0 & 0 & 0 & 0 & 0 & 0 & 0 & 17.03 & 0 \end{bmatrix} \quad (8)$$

$$B = \begin{bmatrix} 0 & 0 & 0 \\ 0 & -2.49 & 2.49 \\ 0 & 0 & 0 \\ 2.87 & -1.43 & -1.43 \\ 0 & 0 & 0 \\ -12.33 & -12.33 & -12.33 \\ 0 & 0 & 0 \\ 0 & 3.56 & -3.56 \\ 0 & 0 & 0 \\ -4.11 & 2.05 & 2.02 \end{bmatrix} \quad (9)$$

### III. CONTROL SCHEME DESIGN

#### A. LQT Control

LQT control theory is a controller design technique that designs an optimal controller by minimizing a quadratic cost function subject to the system dynamics. The state-space model of the ballbot is shown in (5). Define the output error vector:

$$\mathbf{e}(t) = \mathbf{y}_e(t) - \mathbf{y}(t) \quad (10)$$

where  $\mathbf{y}_e$  is the expected output vector.

The optimal control  $\mathbf{u}^*$  is determined by minimizing the quadratic cost function:

$$J = \frac{1}{2} \int_{t_0}^{t_f} [\mathbf{e}^T(t) \mathbf{Q} \mathbf{e}(t) + \mathbf{u}^T(t) \mathbf{R} \mathbf{u}(t)] dt \quad (11)$$

where  $\mathbf{Q}$  and  $\mathbf{R}$  are weighting matrices used to determine the tradeoff between the error and the control effort vectors.  $\mathbf{Q}$  and  $\mathbf{R}$  are positive semi-definite and positive definite matrices respectively. Besides,  $t_0$  and  $t_f$  denote start time and terminal time respectively.

To obtain the optimal control  $\mathbf{u}^*$  by using the minimum principle, we need to construct Hamilton function:

$$\begin{aligned} H &= \frac{1}{2} [\mathbf{e}^T(t) \mathbf{Q} \mathbf{e}(t) + \mathbf{u}^T(t) \mathbf{R} \mathbf{u}(t)] \\ &+ \lambda^T(t) [A \cdot \mathbf{x}(t) + B \cdot \mathbf{u}(t)] \end{aligned} \quad (12)$$

where  $\lambda(t)$  is Lagrangian multiplier vector.

The optimal control  $\mathbf{u}^*$  minimizes the Hamilton function, so it can be computed from the following equations:

$$\begin{cases} \frac{\partial H}{\partial \mathbf{u}} = \mathbf{R} \mathbf{u}(t) + B^T \lambda(t) = 0 \\ \frac{\partial^2 H}{\partial \mathbf{u}^2} = \mathbf{R} > 0 \end{cases} \Rightarrow \mathbf{u}^* = -\mathbf{R}^{-1} B^T \lambda(t) \quad (13)$$

Assume that the solution of  $\lambda(t)$  can be expressed as follows:

$$\lambda(t) = \mathbf{P}(t) \mathbf{x}(t) - \mathbf{g}(t) \quad (14)$$

$$\begin{cases} -\mathbf{P}\mathbf{A} - \mathbf{A}^T\mathbf{P} + \mathbf{P}\mathbf{B}\mathbf{R}^{-1}\mathbf{B}^T\mathbf{P} - \mathbf{C}^T\mathbf{Q}\mathbf{C} = 0 \\ \mathbf{g}(t) \approx [\mathbf{P}\mathbf{B}\mathbf{R}^{-1}\mathbf{B}^T - \mathbf{A}^T]^{-1}\mathbf{C}^T\mathbf{Q}\mathbf{y}_e(t) \end{cases} \quad (15)$$

$$\mathbf{u}^* = -\mathbf{R}^{-1}B^T[\mathbf{P}\mathbf{x}(t) - \mathbf{g}(t)] \quad (16)$$

$$\begin{aligned}\dot{\mathbf{x}} &= A \cdot \mathbf{x} + B \cdot (\mathbf{u} + \mathbf{w}) \\ \mathbf{y} &= C \cdot \mathbf{x} + \mathbf{v}\end{aligned}\quad (17)$$
$$\begin{cases} E[\mathbf{w}\mathbf{w}^T] = Q_N \geq 0 \\ E[\mathbf{v}\mathbf{v}^T] = R_N \geq 0 \\ E[\mathbf{w}\mathbf{v}^T] = 0 \end{cases} \quad (18)$$
$$R_N = 1e-4 \cdot \mathbf{I}[10] \quad (20)$$
$$\begin{aligned}\dot{\hat{\mathbf{x}}} &= A\hat{\mathbf{x}} + B\mathbf{u} + K(\mathbf{y} - C\hat{\mathbf{x}}) \\ \mathbf{u}^* &= L(\mathbf{y}_e - \mathbf{P}\hat{\mathbf{x}})\end{aligned}\quad (21)$$
$$\begin{aligned} \mathbf{G} &= [\mathbf{PBR}^{-1}\mathbf{B}^T - \mathbf{A}^T]^{-1} \mathbf{C}^T \mathbf{Q} \\ \mathbf{L} &= \mathbf{R}^{-1}\mathbf{B}^T \end{aligned} \quad (22)$$


Time (s)	pH <sub>1/2</sub> (deg)
0	10
0.5	0
1	-8
2	-2
3	3
4	1
5	0
6	0
7	0
8	0
9	0
10	0
11	0
12	0
13	0
14	0

Figure 10 is a line graph showing the time response of the yaw angle  $\phi_y$  (in degrees) over a period of 14 seconds. The x-axis is labeled "Time(s)" and ranges from 0 to 14 with major ticks every 2 units. The y-axis is labeled " $\phi_y$  (deg)" and ranges from -15 to 15 with major ticks every 5 units. The curve starts at approximately 10 degrees at  $t=0$ , drops sharply to a minimum of about -8 degrees at  $t \approx 1.5$  s, then rises to a local maximum of about 3 degrees at  $t \approx 3$  s. After this, the curve oscillates with decreasing amplitude, settling near 0 degrees by  $t \approx 6$  s and remaining stable until  $t=14$  s.

Authorized licensed use limited to: Shenyang Aerospace University. Downloaded on March 24, 2021 at 07:20:24 UTC from IEEE Xplore. Restrictions apply.

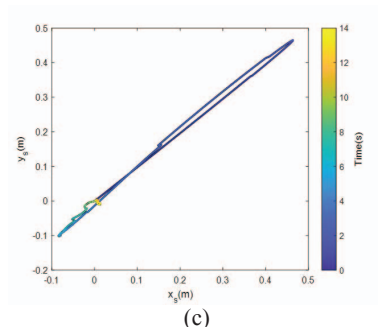
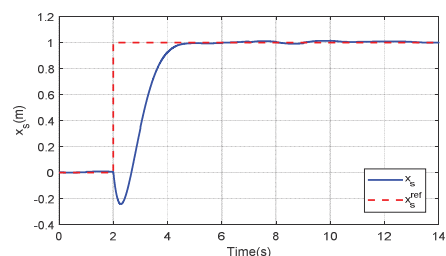
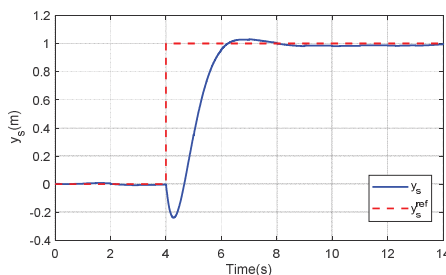


Fig. 5. Simulation results of balancing while station-keeping, (a) Roll angle, (b) Pitch angle, (c) Trajectory of the contact point between the ball and the floor.

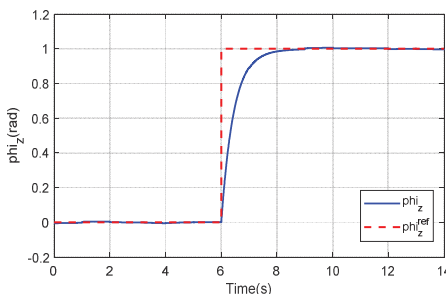
In addition, We simulate the step response of the system. Fig.6(a), (b), (c) show the system response with the changes of  $x_s$ ,  $y_s$  and  $\varphi_z$  at 2, 4 and 6 time units respectively. As we can find the performance of control system, after a transient period, the system can reach the specified position and be stable.



(a)



(b)



(c)

Fig. 6. System response on the change of (a)  $x_s$ , (b)  $y_s$  and (c)  $\varphi_z$ .

## V. CONCLUSION

In this present paper, a structure of the ballbot is introduced. By assuming that the effected noise is white gaussian noise, a Kalman estimator is applied to estimate the internal state of the system using the feedback of inputs. The optimal state-feedback LQT controller is designed to balance and transfer the ballbot system under taking into account the presence of the noise in system states and the output. The simulation results imply the correctness of the system modeling as well as effectiveness of LQT control design for a MIMO ballbot system.

## ACKNOWLEDGMENT

The authors acknowledge the support from the National Key R&D Program of China under grant 2017YFB1300400, the National Natural Science Foundation of China (NSFC) under grant 51875013 and 51575026, and Major Project of the New Generation of Artificial Intelligence(No. 2018AAA0102900).

## REFERENCES

- [1] Pham, Dinh Ba, Jaejun Kim, and Soon-Geul Lee, "Combined control with sliding mode and partial feedback linearization for a spatial rideable ballbot," *Mechanical Systems and Signal Processing*, vol. 128 ,2019, pp. 531-550.
- [2] Kumagai, Masaaki, and Ralph L. Hollis, "Development of a three-dimensional ball rotation sensing system using optical mouse sensors," 2011 IEEE International Conference on Robotics and Automation. IEEE, 2011, pp. 5038-5043.
- [3] Asgari, Pouya, and S. Ali A. Moosavian, "Dynamics modeling and control of an armed Ballbot with stabilizer," 2013 First RSI/ISM International Conference on Robotics and Mechatronics, IEEE, 2013, pp. 236-241.
- [4] Shomin, Michael, Jodi Forlizzi, and Ralph Hollis, "Sit-to-stand assistance with a balancing mobile robot," 2015 IEEE International Conference on Robotics and Automation, IEEE, 2015, pp. 3795-3800.
- [5] Cai, Chengtao, Jiaxin Lu, and Zuoyong Li, "Kinematic analysis and control algorithm for the Ballbot," *IEEE Access*, vol. 7, 2019, pp. 38314-38321.
- [6] Nagarajan, Umashankar, George Kantor, and Ralph Hollis, "The ballbot: An omnidirectional balancing mobile robot," *The International Journal of Robotics Research*, vol. 33.6, 2014, pp. 917-930.
- [7] Kumaga, Masaaki, and Takaya Ochiai, "Development of a robot balanced on a ball—Application of passive motion to transport—," 2009 IEEE International Conference on Robotics and Automation, IEEE, 2009, pp. 4106-4111.
- [8] Pham, Dinh Ba, and Soon-Geul Lee, "Hierarchical sliding mode control for a two-dimensional ball segway that is a class of a second-order underactuated system," *Journal of Vibration and Control*, vol. 25.1, 2019, pp. 72-83.
- [9] Fankhauser, Peter, and Corsin Gwerder, *Modeling and control of a ballbot*, BS thesis, Eidgenössische Technische Hochschule Zürich, 2010.
- [10] Alstrin, André, and Emil Sundell, *Development of a mechatronical platform for AUTOSAR-The ball-balancing robot*, MS thesis, 2015.
- [11] Blonk, J. W., *Modeling and control of a ball-balancing robot*, MS thesis, University of Twente, 2014.
- [12] Lee, Soon-Geul, "LQG control design for a coupled ballbot dynamical system," 2018 18th International Conference on Control, Automation and Systems, IEEE, 2018, pp. 666-670.